Spontaneous Symmetry Breaking Turing-Type Pattern Formation in a Confined *Dictyostelium* Cell Mass

Satoshi Sawai,[1] Yasuo Maeda,[2] and Yasuji Sawada[3]

[1]*Graduate School of Information Sciences, Tohoku University, Katahira, Sendai 980-8577, Japan*
[2]*Biological Institute, Graduate School of Science, Tohoku University, Aoba, Sendai 980-8578, Japan*
[3]*Research Institute of Electrical Communication, Tohoku University, Katahira, Sendai 980-8577, Japan*

(Received 26 January 2000)

We have discovered a new type of patterning which occurs in a two-dimensionally confined cell mass of the cellular slime mold *Dictyostelium discoideum*. Besides the longitudinal structure reported earlier, we observed a spontaneous symmetry breaking spot pattern whose wavelength shows similar strain dependency to that of the longitudinal pattern. We propose that these structures are due to a reaction-diffusion Turing instability similar to the one which has been exemplified by CIMA (chlorite-iodide-malonic acid) reaction. The present finding may exhibit the first biochemical Turing structure in a developmental system with a controllable boundary condition.

PACS numbers: 87.18.Hf, 05.65.+b, 47.54.+r

In a system far from equilibrium, a stationary periodic structure can self-organize from an initially uniform state when diffusion couples long range inhibition and short range activation of two chemical species. In the Turing instability, a spatial pattern of reactant concentration develops from a very small perturbation (see [1] for the mathematical formalism). This was first theoretically introduced by Turing in 1952 to explain how patterns during morphogenesis are generated [2]. Only recently, in 1990, were such patterns experimentally demonstrated using a chemical gel-reactor [3,4].

The uniqueness of this mechanism lies in the pattern's spontaneous symmetry breaking with a characteristic wavelength solely determined by kinetics and diffusion. All other nonequilibrium pattern formations such as Rayleigh-Bénard convection, create structures that depend on the global geometry. Especially in morphogenesis, where robustness of a spatial pattern to external or internal disturbances is frequently observed, the Turing mechanism is the most plausible physical basis [1,5].

Supported by both quantitative and qualitative experimental data, though the molecular details are still unknown, evidence has accumulated in recent years that formation of certain pigment patterns [6] and morphogenetic prepatterns [7–10] is dictated by the Turing instability. In biological systems, however, owing to cell heterogeneity and tissue asymmetry, it is usually not possible to study a homogeneous experimental system with controllable boundary conditions. Thus there still remained some uncertainty to conclude the mechanism behind such biological pattern formation.

The cellular slime mold *Dictyostelium discoideum* avoids many potential difficulties, since cells develop from almost homogeneous vegetative phase cells without significant cell division. When starved and dispersed on an agar plate, cells aggregate to form a mound structure by chemotaxing towards propagating cAMP waves in a well-characterized example of self-organization [11]. Cells then form a moving body structure called pseudoplasmodium, often referred to as a slug. The anterior portion, about one-fourth of the total volume consists of prestalk cells which later form the vacuolated stalk of the fruiting body. The cells in the posterior region are prespore cells which later become spores [12]. The initial cell-type differentiation starts at the early mound stage. Prestalk cells differentiate position dependently within the mound and later sort out to form the tip of a slug [13].

Bonner *et al.* discovered that when *D. discoideum* cells are trapped in a glass capillary and sealed with mineral oil at one end, leaving the other end open, a dark band emerges within several minutes at the open end [14]. Cells in the dark zone show active random movement and can be stained with neutral red which serves as a prestalk marker. Cell-type specific gene expression detected with a GFP (green fluorescent protein) transformant suggested that these cells differentiate into a prestalk subtype. Cells in the interior zone are motionless and seem to dedifferentiate [15].

What type of dynamics is responsible for this particular pattern formation? The length of the dark zone is independent of system size and remains essentially unchanged below a certain boundary oxygen concentration [16]. When 1D capillary experiment is conducted by a small volume of cells with both sides opened to the air, dark zones are initially established at both ends, but one of them slowly disappears during the next several hours [17]. The observed lateral inhibition suggests that the underlying kinetics of the patterning exhibits a Turing-type instability. High oxygen concentration in the outer region is considered to act as a trigger to enhance autocatalytic production of a darkening agent which simultaneously induces elevation of another agent that diffuses much faster and inhibits the darkening reaction by the cells in the neighboring region. Such kinetic mechanism of the patterning is also supported by the fact that the effect of temperature T on zone size L_{out} follows $\ln L_{\text{out}} \propto 1/T$ in accordance with the

 0031-9007/00/85(10)/2212(4)$15.00

Arrhenius law for underlying kinetic constants [18]. These strongly suggest that the pattern is generated by the reaction diffusion of an activator and an inhibitor. In this Letter, we demonstrate that spontaneous symmetry breaking takes place when a planar cell mass is provided with oxygen in the vertical direction through porous glass.

D. discoideum NC-4 and Ax-2 cells were grown according to the standard procedures [19,20]. The two-dimensionally confined cell mass was prepared as described in Ref. [16] with a minor change. Washed cells were pelleted by centrifugation and layed on a slide glass along with two spacers of approximately 100 μm thickness. Instead of a cover glass, porous glass (1.58 mm thickness, Vycor 7930) saturated with Bonner's salt solution [19] was layed on top of the cell mass and the spacers. We kept samples in a plastic plate together with wet paper towels to maintain the humidity above 95%. Measurements were performed with an Olympus IMT-2 microscope equipped with a Sony CCD-IRIS camera.

We observed patterns within the circular cell mass confined between two glass slides. The pattern during the first 30 minutes has the same wavelength and texture with either a normal or a porous glass top-cover. Figure 1(a) displays the pattern observed as a clear difference in the level of transmitted light. Cells in the outer zone rapidly turn dark, while cells farther inside remain unchanged. The border between these two regions is strikingly sharp with almost no transport of cells across it.

The length of the zone L_{out} was measured for samples ranging from approximately 450 to 2000 μm in diameter under the normal glass (data not shown). L_{out} at atmospheric oxygen concentrations is system-size independent but strain dependent; $L_{\text{out}} = 145 \pm 7$ μm and 110 ± 4 μm for strains Ax-2 and NC-4, respectively. Since the observed wavelength is close to that of the spacer thickness, we also confirmed that the length does not differ for other spacer thicknesses (50 and 200 μm). It has also been demonstrated with NC-4 cells that the patterning with the same characteristic length occurs even with a thickness close to a monolayer (25 μm) [16]. The pattern size seems to be independent of the geometry of the experiment.

To check the strain dependence on other controllable parameters, we measured the wavelength with a continuous supply of a mixture of oxygen and nitrogen gas kept at a constant flow-rate ratio. After an initial transient of approximately 1 h, we calculated the time average at several times over 30 min to 1 h time periods. Figure 2 shows that the zone length becomes very weakly dependent on oxygen concentration below 20%. Surprisingly, the pattern persists even down to an oxygen concentration of 0.6%. The difference of L_{out} between the two strains increased with oxygen concentration (see [16] for the NC-4 measurement). However, close to onset, the zone length was approximately 70 μm for both. We conclude that, as oxygen concentration is lowered, the size of the stationary front approaches a characteristic length which is not strain dependent.

When using porous glass, unlike normal glass, a drastic transition occurs 30–60 min after sample preparation. This is attributed to the altered boundary conditions with oxygen provided vertically through the porous glass.

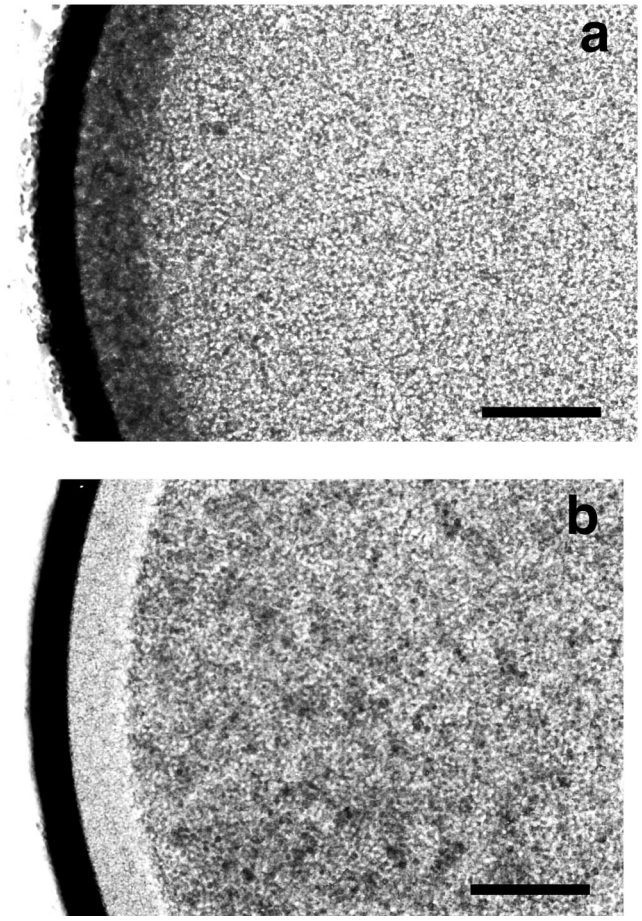

FIG. 1. Initial evolution of the pattern under a porous glass top cover. Snapshots are taken at (a) $t = 12$ min and (b) 54 min. Scale bars show 150 μm. The outermost black shade is a meniscus. See text for details.

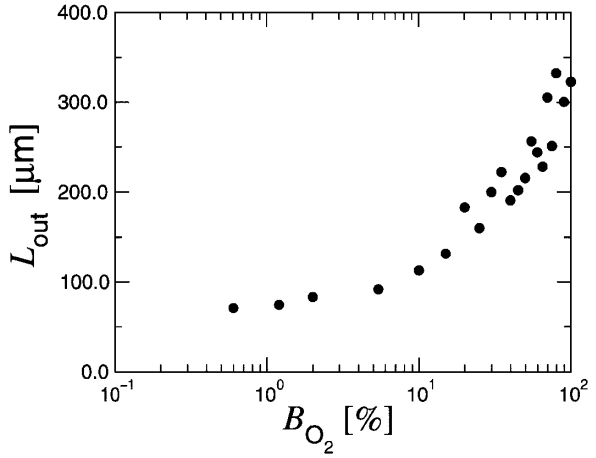

FIG. 2. Boundary oxygen concentration B_{O_2} and the dark zone length L_{out}. Ax-2 cells were used and the temperature was kept at 22 °C. See text for details.

Darkening of cells similar to that observed in the periphery occurs throughout the inner zone. The delay is most likely due to the limited diffusion rate of oxygen through the porous glass. The outer dark zone turns bright almost simultaneously. The inner dark zone then slowly becomes inhomogeneous in contrast [Fig. 1(b)], giving rise to a spontaneous symmetry breaking spot pattern (Fig. 3) which persists for more than 10 hours until cells in the outer zone form slugs. Cells that constitute dark spots show random fluctuating motion as do those in the longitudinal dark zone. Peaks in Fig. 4 show the characteristic distance λ between the spots seen in Fig. 3(a), determined by a spatial autocorrelation of the gray scale in Fig. 3(a) calculated as a function of $r = \sqrt{x^2 + y^2}$. We have obtained λ for both strains and found $\lambda = 143 \pm 4$ μm for Ax-2 and $\lambda = 100 \pm 10$ μm for NC-4. The strain dependence resembles that in the longitudinal case.

The present results could most easily be interpreted by a process analogous in dynamics to the purely chemical reaction-diffusion process, since they show characteristics of the Turing instability, namely, that the cell mass is able to go through a spontaneous symmetry breaking and give rise to a stationary periodic structure with a characteristic size independent of the system geometry. During both the longitudinal and the spot pattern formation, time-lapse video recording revealed no pulsatile directed cell movement nor streaminglike cell aggregation typical at the aggregation stage. Dark cells merely show active uncoordinated motion without much translocation. Formation of the spot pattern also indicates that the pattern is not due to a mere switching of cells between two physiological states responding to whether they are above or below an oxygen threshold. The pore diameter of the glass is $\sim$4–6 nm in average [21], therefore too small to explain the spot size. Moreover, if cells sense a threshold of oxygen, the longitudinal pattern should converge to a size close to one cell diameter and eventually drop to zero. However, the trend of the curve in Fig. 2 at extreme anoxia environment suggests that the zone length converges to as much as 5 times longer than a cell diameter.

The longitudinal pattern extending in a direction parallel to the imposed oxygen gradient is not a symmetry breaking pattern. Although the origin of such longitudinal patterns is not well studied in chemical systems, some could be of Turing-type. Experimental and numerical studies show that a stationary front, similar to the one observed,

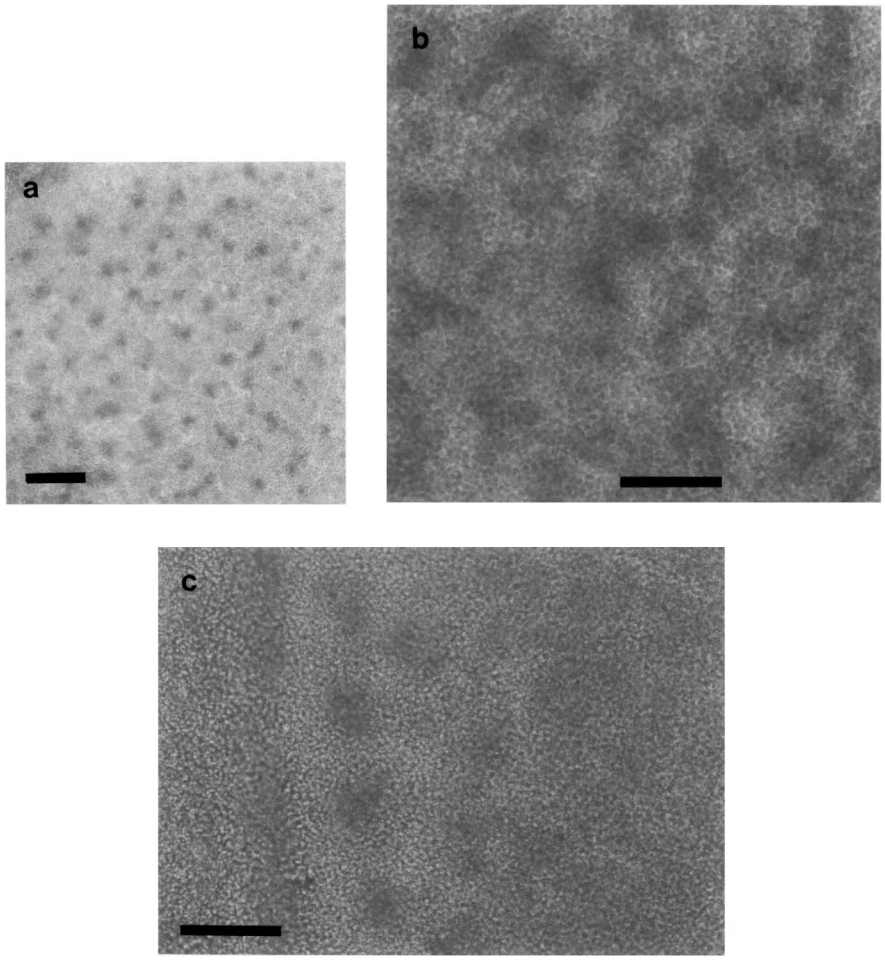

FIG. 3. Symmetry breaking pattern observed under porous glass top cover. (a),(c) Ax-2 cells at $t = 10$ h and (b) NC-4 cells at $t = 6$ h. The cell mass was prepared and observed at 22 °C in atmospheric oxygen environment. Scale bars: (a) 200 μm, (b) 100 μm, and (c) 150 μm.

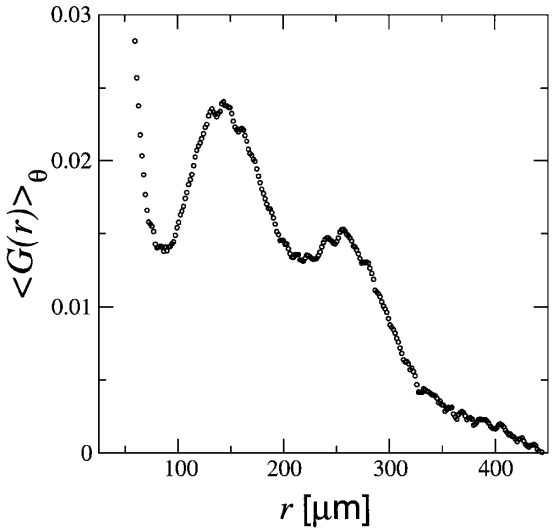

FIG. 4. Spatial autocorrelation showing the characteristic size of the spot pattern; calculated from the gray-scale image in Fig. 3(a).

develops along the feeding surface in boundary-fed reaction-diffusion systems [22]. Pattern selection of such localized structures depends on the steepness and the exact form of the imposed spatial variation of the control parameter. A pattern resembling a hexagon-stripe competition is observed near the border, as shown in Fig. 3(c), where spots line up parallel to the longitudinal front.

The apparent convergence of the longitudinal pattern to a characteristic length and its strain independence suggest that lowering of oxygen concentration brings the system close to a bifurcation point. A very small amount of oxygen is enough to initiate the nonlinear reaction-diffusion mechanism. As the system is driven away from the onset, nonlinearity increases and alters the wavelength selection curve strain dependently. At very high oxygen concentrations, though stationary, the longitudinal pattern possesses multimodal characteristics (see Fig. 2), suggesting a delicate hysterises and a competition between sideband modes.

The cells in the dark spot as well as in the dark band are certainly more active than the cells in the other zone. We believe that such difference in the motility is not the cause but the consequence of the patterning. A rapid change in the cytosolic *p*H and Ca2+ is observed during the patterning [14,18]. Darkening of cells may be reflecting such physiological alteration within the cytosol, causing reversible rearrangement of some cortical cytoskeletal filaments. The cells in the longitudinal dark zone eventually form slugs in the later stage, therefore they do not simply correspond to prestalk cells as was discussed previously [14,16]. A study on the relation between the patterning and position dependent cell-type differentiation will be presented elsewhere [15].

The system has advantages of physically controlling biological pattern formation and following it in 2D. The geometry of the experiments resembles that of the CIMA (chlorite-iodide-malonic acid) reaction experiments in a gel strip or disk [3,4] which also allow observations of the transverse patterns in a plane perpendicular to the source feed gradient. The similarity of some of the results between our system and the CIMA reactors should be worth further detailed study.

We thank T. Hirano and L. F. Jaffe for their continuing interests toward this and related studies. We also thank Y. Hayakawa for an image format conversion; J. A. Glazier for suggestions on our earlier draft, and E. C. Cox for pointing out the pioneering works.

[1] J. D. Murray, *Mathematical Biology* (Springer-Verlag, Berlin, 1989), p. 435.
[2] A. M. Turing, Philos. Trans. R. Soc. London B **237**, 37 (1952).
[3] V. Castets *et al.,* Phys. Rev. Lett. **64**, 2953 (1990).
[4] Q. Ouyang and H. L. Swinney, Nature (London) **352**, 610 (1991).
[5] H. Meinhardt, *Models of Biological Pattern Formation* (Academic, New York, 1982), p. 12.
[6] S. Kondo and R. Asai, Nature (London) **376**, 765 (1995).
[7] L. G. Harrison *et al.,* Protoplasma **106**, 211 (1981).
[8] J. G. McNally and E. C. Cox, Development **105**, 323 (1989); K. Gregg, I. Carrin, and E. C. Cox, Dev. Biol. **180**, 511 (1996).
[9] S. C. Smith and J. B. Armstrong, Dev. Biol. **160**, 535 (1993).
[10] M. Sato, H. R. Bode, and Y. Sawada, Dev. Biol. **141**, 412 (1990); H. Shimizu, Y. Sawada, and T. Sugiyama, Dev. Biol. **155**, 287 (1993).
[11] Y. Jiang, H. Levine, and J. Glazier, Biophys. J. **75**, 2615 (1998); H. Levine, L. Tsimring, and D. Kessler, Physica (Amsterdam) **106D**, 375 (1997); J. C. Dallon and H. G. Othmer, Philos. Trans. R. Soc. London B **352**, 391 (1997); K. J. Lee, E. C. Cox, and R. E. Goldstein, Phys. Rev. Lett. **76**, 1174 (1996).
[12] *Dictyostelium A Model System for Cell and Developmental Biology,* edited by Y. Maeda, K. Inouye, and I. Takeuchi (Universal Academy Press, Tokyo, 1997).
[13] A. Early, T. Abe, and J. Williams, Cell **83**, 91 (1995).
[14] J. T. Bonner *et al.,* Proc. Natl. Acad. Sci. U.S.A. **92**, 8249 (1995). Cytosolic calcium change during the patterning is documented in M. Azhar and V. Nanjundiah, J. Biosci. **21**, 765 (1996); L. F. Jaffe, in Ref. [12], p. 267.
[15] T. Hirano *et al.,* Dev. Growth Differ. (to be published).
[16] Y. Sawada *et al.,* Dev. Growth Differ. **40**, 113 (1998).
[17] J. T. Bonner, L. Segel, and E. C. Cox, J. Biosci. **23**, 177 (1998).
[18] S. Sawai *et al.* (to be published).
[19] J. T. Bonner, J. Exp. Zool. **106**, 10 (1947).
[20] D. J. Watts and J. M. Ashworth, Biochem. J. **119**, 171 (1970).
[21] T. H. Elmer, Engineered Materials Handbook **4**, 427 (1992).
[22] G. Dewel *et al.,* Physica (Amsterdam) **213A**, 181 (1995); P. Borckmans, A. De Wit, and G. Dewel, Physica (Amsterdam) **188A**, 137 (1992); A. De Wit, G. Dewel, P. Borckmans, and D. Walgraef, Physica (Amsterdam) **61D**, 289 (1992).